
Hypothesis Generation and Inductive Inference in Children and Language Models

Jeffrey Qin

Computer Science
University of Waterloo
jzqin@uwaterloo.ca

Wasu Top Piriyakulkij

Department of Computer Science
Cornell University
wp237@cornell.edu

Zhuangfei Gao

Department of Computer Science
Dalhousie University

Mia Radovanovic

Department of Psychology
University of Toronto

Jessica Sommerville

jessica.sommerville@mail.utoronto.ca
Department of Psychology
University of Toronto

Kevin Ellis

Department of Computer Science
Cornell University
kellis@cornell.edu

Marta Kryven

Department of Computer Science
Dalhousie University
marta.kryven@dal.ca

Abstract

Real world decision-making requires constructing mental models under uncertainty over evidence, over the underlying causal rules, and over the state of the world itself. Which computational principles underpin human inference under such conditions, and do LLM-based agents exhibit similar behavior given matching constraints? We address these questions using an inductive inference Box Task in which participants – human children and LLM-based agents – infer a latent cause through sequential interaction with an uncertain environment. We formalize this task as program induction with Bayesian particle-based inference, admitting two complementary interpretations: (1) as a constraint satisfaction process over hypotheses, and (2) as a program synthesis problem in which hypotheses are executable programs evaluated against evidence. Using the constraint-based formulation, we show that children’s behavior is best explained by a combination of subjective evidence reliability and online hypothesis generation, accounting for both their evidence-seeking patterns and their dissociation between task completion and rule generalization. Using the program synthesis formulation, we treat LLM-based agents as *model organisms*: controllable systems that allow systematic manipulation of task conditions. Across backends, LLM-based agents replicate children’s responses to changes in evidence reliability and observability, including discounting unreliable evidence, seeking to resolve partial information, and dissociating between task completion and causal generalization. At the same time, LLM-based agents tend to over-observe and over-comply with instructions relative to children. These results suggest that while children and LLM-based agents adapt similarly to environmental structure, their information-seeking behavior exhibits distinct underlying costs and inductive biases.

1 Introduction

When Newtonian mechanics subsumed Aristotelian physics, it marked a shift from a framework of motion governed by heterogeneous causes to a unified theory of inertia and force. This transition illustrates the effectiveness with which humans iteratively construct complex causal models via revision and experimentation [19]. Identifying the computational principles that enable agents to discover coherent theories under real-world conditions remains a key challenge in cognitive science [36], robotics [8], and model interpretability [40].

A central obstacle to the controlled study of real-world inference is the presence of interacting sources of uncertainty, and scarcity of experimental frameworks that systematically vary them across systems [40, 1]. Here, we address this challenge through a computational study of human behavior in a physical puzzle-solving domain, and using formal modeling to characterize the computational principles underlying behavior. We extend this analysis to large language models (LLMs), treating them as *model organisms* that enable systematic variation of environmental conditions [12, 34]— to examine how these principles shape human and machine inference under matched constraints.

We develop our framework by modeling behavior in the Box Task [30], an inductive inference paradigm originally designed to study how 7-10 year old children respond to misleading instructions under uncertainty. Children constitute ideal subjects for our goal, as unlike adults, they approach inference with minimal prior knowledge, making their behavior more sensitive to the task structure [14, 15]. The Box Task requires participants to open five physical locked boxes using thirteen keys in limited time. To do this successfully, participants need to discover a latent rule governing key–box combinations by interpreting symbols shown on key fobs and box faces (Figure 1A). The Box Task is partially observable, because not all box faces are visible without picking up a box; it features unreliable evidence, as physical malfunction of the key-lock mechanism can prevent a ‘correct’ combination from opening. At a computational level [25], shared by children, cognitive models, and artificial agents, this process constitutes a partially observable Markov decision process (POMDP) where the agent must discover a latent rule given stochastic state transitions and incomplete observations. At the representation level, we draw on recent work in world model learning [35, 27] to approximate the solution using program induction with particle-based Bayesian inference.

Our framework admits two complementary implementations. The first, Sets of Constraints (SoC), represents hypotheses as structured collections of evidence-derived constraints and serves as a cognitive model fit to children’s behavior. The second, LLM-based Program Synthesis (LLM-PS), represents hypotheses as executable programs generated and revised by an LLM, enabling tractable inference in a flexible hypothesis space. Here SoC functions to identify which cognitive principles drive human behavior, while LLM-PS provides a controllable system for probing how behavior changes under their systematic variation.

Across these implementations, we find that children and LLM-based agents respond similarly to changes in evidence reliability and partial observability, but differ systematically in how they trade off information, reliability, and generalization. In particular, children tend to under-observe and often fail to generalize despite solving the task, whereas LLM-based agents tend to over-observe, leading them to more readily recover the underlying rule.

We contribute the following:

1. **A formalization of inductive inference** admitting two complementary implementations as constraint-based (SoC) and as program synthesis (LLM-PS) — extending the Sampling Hypothesis [11] to settings with unreliable evidence and unbounded hypothesis spaces.
2. **A computational analysis of children’s inference under uncertainty** showing that subjective evidence reliability and online hypothesis generation jointly account for children’s behavior, including the dissociation between task completion and true-rule generalization.
3. **A controlled comparison between children and LLM-based agents.** Treating LLM-based agents as *model organisms*, we systematically vary evidence reliability and observability, showing that LLM-based agents replicate children’s performance patterns in uncertain conditions, but express diverging inductive biases.

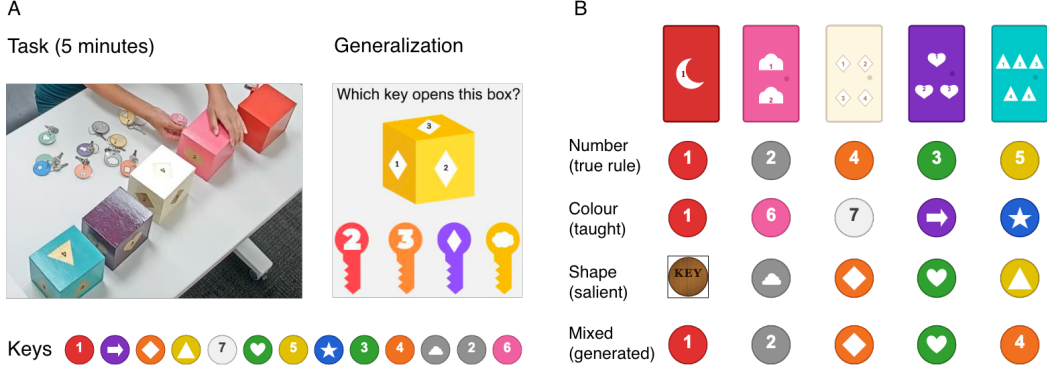


Figure 1: A. Children were presented with 5 locked physical boxes and 13 keys, and asked to open them within 5 minutes. Next, children completed four generalization trials presented on a screen, showing a previously unseen box and a new set of keys. B. The true (fully observed) set of boxes, along with four hypothetical SoC that could open them. *Number* (the true rule) shows the actual key-box mapping. *color* represents the taught (misleading) rule. *Shape* rule assumes that any key could open the first box, which has no matching shape key, while other boxes are matched by shape. *Mixed* shows an example of a SoC generated online, which sampled boxes and keys based on salient properties. All four rules are consistent with red key opening the red box.

2 Methods

2.1 The Box Task

The Box Task [30] is a naturalistic inductive inference paradigm in which 7-10 year old children ($N = 100$) were given 5 minutes to open 5 closed boxes using 13 keys. Boxes are uniquely colored, each marked with multiple instances of a single shape, and presented in a fixed order. Keys have colored fobs displaying either a shape or a number. The true rule, unknown to children, is that each box opens with the key whose number matches the number of shapes on the box (Figure 1A).

Children are deliberately misled: Before commencing the task, children viewed a video in which a teacher misleadingly instructed them that boxes open with color-matching keys. The task is partially observable: shapes on box sides are not visible without picking up the box. Children may pick up the boxes to examine them. Following the task, children completed four generalization trials selecting which of four new keys would open an unseen box, where one of the keys corresponds to the true rule and the other three keys are foils. Although 66% of children opened all five boxes, only 22% generalized the true rule [30] — reflecting the difficulty of rule inference. Full description of the procedure is given in Appendix A.

2.2 POMDP Formalization

The Box Task defines a partially observable inference problem: the agent must discover a latent rule h from evidence that is both unreliable and incomplete. We formalize this as a POMDP to characterize the structure of the problem faced by all agents, including children and artificial agents, before describing how each implementation approximates it.

Formally the Box Task is a POMDP in which the state $s = (n_1, \dots, n_5, o_1, \dots, o_5, h)$ encodes the number of shapes on each box $n_i \in \{1, \dots, 5\}$, whether each box is open $o_i \in \{0, 1\}$, and the rule (hypothesis) h predicting which key opens each box. The open indicators o_i are fully observable. The numbers n_i can be observed by picking up each box. The rule h is never observed directly. The reward $r = 1$ when $\forall i o_i = 1$, and 0 otherwise. The task terminates when $\sum_i o_i = 5$.

Action space. At each step, the agent chooses between two action types:

- **OBSERVE(i):** reveals information about n_i , reducing uncertainty on box i .
- **ATTEMPT(i, j):** attempts to open box i with key j ; succeeds if the oracle rule predicts a match, subject to evidence reliability ρ .

State transitions. OBSERVE(i) deterministically reveals n_i and o_i but leaves h unchanged. The revealed n_i value may update belief over h if it is consistent with evidence accumulated from prior attempts. ATTEMPT(i,j) produces a binary outcome $y \sim \text{Bernoulli}(\rho)$ if h predicts success, and $y = 0$ otherwise. When $y = 1$, the state transitions to $o_i = 1$. Because $\rho < 1$, a correct attempt may fail, and a failed attempt on an opened box is not fully informative about h . Both action types can in principle update belief over h : Attempt outcomes do so directly via likelihood weighting; Observe outcomes do so indirectly when the revealed n_i is consistent with or contradicts accumulated attempt evidence.

Updating beliefs. Since o_i is fully observable, the belief reduces to a joint distribution over shape counts and latent rule: $b = p(n_1, \dots, n_5, h \mid \text{history})$. This belief has two interacting sources of uncertainty over number and rule.

Exact maintenance of the joint belief $p(n_{1:5}, h \mid \text{history})$ is intractable [20], and our two implementations approximate this belief in different ways. SoC marginalizes over number uncertainty and maintains a particle distribution solely over $p(h)$; OBSERVE(i) actions are not explicitly modeled for children. LLM-PS-P factorizes the belief state for each $p(n_i)$, representing it as a set of candidate values, initialized to encode all possible values. This can be collapsed using OBSERVE(i) actions. Further, the rule hypothesis h is an executable program, that can use predicate `box.number` $\in N_i$ to operate over this set.

2.3 Probabilistic inference framework

We model inductive inference as online Bayesian updating over a distribution of causal hypotheses, implemented using Sequential Monte Carlo Samplers (SMC-S; [10]). We follow the SMC Samplers formulation of [10], which is suited to settings where the posterior at each timestep shares a common hypothesis space — as is the case here. At each trial t , the agent maintains a population of N hypothesis particles $\{h_t^i, w_t^i\}_{i=1}^N$, where h_t^i is a hypothesis and w_t^i its weight. An approximate posterior over hypotheses given history of actions $e_{1:t} = (\text{key}, \text{box})$ and observed outcomes $y_{1:t} \in \{0, 1\}$ is:

$$p(h \mid e_{1:t}, y_{1:t}) \approx \sum_i w_t^i \mathbb{1}[h = h_t^i].$$

Hypotheses are generated by a proposal distribution $q(h)$, described separately for each implementation below.

Action selection. At each step, the agent selects the key-box pair e^* maximizing expected information gain over the current particle distribution [24, 31]:

$$e^* = \arg \max_{e \in \mathcal{E}} \sum_i w_t^i \mathbb{E}_{y \sim p(\cdot \mid e, h_t^i)} \left[D_{\text{KL}} \left(p(h \mid e_{1:t}, y_{1:t}, e, y) \parallel p(h \mid e_{1:t}, y_{1:t}) \right) \right].$$

Belief updating. Upon observing outcome y_t of action e_t , particle weights are updated:

$$w_t^i \propto w_{t-1}^i \cdot p(y_t \mid e_t, h_t^i).$$

To model uncertainty over *evidence reliability* as the tendency to attribute failures to external causes (e.g., a stiff lock) rather than immediately falsifying the hypothesis, we introduce a *subjective reliability* parameter $\rho \in (0, 1]$: Then, the likelihood is Bernoulli with success rate ρ when h predicts success and 0 otherwise:

$$p(y \mid e, h) = \text{Bernoulli}(y; \rho \cdot \mathbb{1}[h \text{ predicts } e \text{ succeeds}]).$$

Importantly, while the key behavior may objectively be stochastic, here ρ reflects the agent’s subjective estimate of how reliable keys are. Empirical support for this assumption comes from two observations in children’s behavior: key success rates fall below 1.0 across all children, and children frequently retry the same key–box pair on consecutive trials despite prior failure, consistent with attributing failures to physical causes rather than rule mismatch (figures are shown in AppendixD.3).

Resampling and rejuvenation. When the effective sample size $ESS = 1 / \sum_i (w_t^i)^2$ falls below $N/2$, particles are resampled proportionally to their weights and rejuvenated by drawing from $q(h)$ to restore diversity. The rejuvenation mechanism is representation-specific, described separately for SoC and LLM-PS below.

SMC-S aligns with the computational cognitive principles expressed in the Sampling Hypothesis [11], as it can be configured to track a small set of hypotheses to account for bounded rationality constraints [33]. It also captures the incremental nature of human learning where evidence arrives over time, and beliefs evolve one time step to the next. The two implementations of this inference machinery below differ in how hypotheses h are represented and how the proposal distribution $q(h)$ generates and refines them. SoC establishes which computational principles are required to account for human behavior. LLM-PS establishes what those principles do by probing their effects under controlled variation.

2.3.1 Hypotheses as Sets of Constraints (SoC)

Each hypothesis h^i is a *Set of Constraints* (SoC): a mapping of boxes to keys predicted to open them. Examples of such sets, including the true rule and the taught color rule are shown in Figure 1 B. The initial particle population is drawn from $q(h)$, structured as a mixture of two components:

- **Pre-specified rules:** Following the Sampling Hypothesis – a currently standard mechanistic approach in the causal learning literature [11] – we specify a set of salient candidate rules matching by color, shape, or box order, each assigned a prior probability $p(h)$. The prior probability of the true rule is a free parameter of the model, p_t , fit to behavior.
- **Online generator:** A generative mechanism for proposing novel SoCs not in the pre-specified set, implemented by uniform sampling of key-box assignments conditioned on accumulated evidence: assignments consistent with observed successes are upweighted, while assignments that have been falsified are downweighted in proportion to their accumulated failure probability under the current reliability estimate ρ . A parameter p_{gen} controls the proportion of prior mass allocated to the generator versus pre-specified rules.

Particles are initialized with weights $w_1^i \propto p(h_1^i)/q(h_1^i)$, reducing to uniform weights when priors are sampled directly. After resampling, diversity is restored by drawing fresh samples from $q(h)$ and adding them to the particle pool.

Model variants. We construct four SoC variants, including three lesioned versions:

1. **Lesioned (SoC-L)**, reliable evidence and no generator ($\rho = 1, p_{gen} = 0$).
2. **Subjective reliability only (SoC-Rel)**, no generator ($p_{gen} = 0$)
3. **Generator only (SoC-Gen)**, no subjective reliability ($\rho = 1$)
4. **Full model (SoC-Full)**, all the parameters p_{gen}, ρ and p_t are present

2.3.2 Hypotheses as Symbolic Programs (LLM-PS)

Hypotheses h^i are represented as executable Python functions `predict(key, box) -> bool`, evaluated against evidence as test cases. The initial particle population is generated by prompting the LLM with a description of the Box Task environment, the misleading instruction as a starter hypothesis, and a code template specifying Key and Box data structures. Each particle is an independently sampled program consistent with this context. When a particle h^i is selected for rejuvenation, the LLM is prompted to synthesize a revised version of the corresponding hypothesis consistent with accumulated evidence. This inference machinery determines *which* hypotheses to revise and *when*, while the LLM determines *how*, which distinguishes LLM-PS from pure prompt engineering.

Model variants. To isolate the computational contributions of evidence reliability and partial observability, we implement four model variants, each corresponding to a distinct environmental condition :

LLM-PS, full observability, reliable keys: The LLM receives a complete description of the environment, including full specification of all boxes describing the symbols and numbers on each face. Keys succeed deterministically when attempting to open the correct box.

LLM-PS-S, full observability, unreliable keys: Evidence reliability is degraded to match empirical success rates experienced by children (see Appendix D.3).

LLM-PS-P, partial observability, unreliable keys: Box face counts are not provided; the agent may issue `OBSERVE(i)` actions to reveal them. Keys remain unreliable.

The prompts (shown in Appendix B) are determined by task conditions; the number of particles is a free parameter of the model (fewer particles converge faster); LLM back-end used as a proposal distribution is another free parameter (more capable models need fewer particles). Neither was fitted to behavioral data. Unlike SoC, which we use as a principled model of human behavior, LLM-based agents serve as model organisms to understand how artificial agents respond to variation in environmental conditions. Unlike SoC, that uses EES on the rejuvenation step, LLM-PS rejuvenates the worst hypothesis at every trial [27]. In addition to these model variants, we implement a **ReAct [39] baseline**: LLM prompted sequentially with evidence history and prompted to produce key-box actions directly, without generating explicit hypotheses. The ReAct operates in a fully observable environment with reliable keys, serving as an unstructured baseline: capable of completing the task, but without producing interpretable hypotheses or generalization to unseen boxes. We use the four model configurations with several LLM backends with different architectures, showing that they achieve different results, yet respond similarly to increasing difficulty in the environment.

Action selection under partial observability. In LLM-PS-P, `OBSERVE(i)` actions are not evaluated under the EIG criterion, but when issued, they update the environment context passed to subsequent LLM calls. Particles generated prior to observation retain their original representation and may be discarded through subsequent rejuvenation; particles generated after observation can exploit the revealed count directly. This implements a factorized approximation to the joint belief $p(n_{1:5}, h \mid \text{history})$, treating state uncertainty and rule uncertainty as an independent tractable approximation of the formalism described in Section 2.2.

3 Experiments

3.1 SoC Results

We evaluate the SoC model’s ability to capture children’s causal learning in the Box Task by focusing on two core behavioral signatures: (1) the model’s ability to predict children’s trajectories of opening attempts, and (2) the final causal hypothesis inferred by the model.

We fit each model variant using Maximum Likelihood Estimation (MLE). Parameter selection is done separately for each child i by maximizing log-likelihood (LL) of that child’s trajectory given each model’s predictions. We then select the best fitting model for each child as the model with the highest LL (Figure 2B) and report the population mean LL for each model (Figure 2C) to assess model fit. Both approaches identify SoC-Full as the best fitting model. The Full model provides a significantly better fit than all lesioned variants ($p < .001$): SoC-Rel ($t = 13.39, d = 1.34$), SoC-Lesioned ($t = 10.14, d = 1.01$), and SoC-Gen ($t = 3.90, d = 0.39$). AIC-based model comparison confirms this ranking after penalising for model complexity (Appendix C, Table 4). Figure 2(a) shows histograms of trials required to open all five boxes for each model variant alongside children’s distribution, showing that the SoC-Full model closely reproduces the shape and spread of children’s aggregate distribution, in contrast to lesioned variants.

The bottom row of Figure 2 shows the distribution of final inferred rules. Children generalized the true rule at 22%; the Full model converges on the correct rule in approximately 20% of simulations, matching children’s generalization rate. This convergence, alongside the lesion results, establishes that subjective reliability (ρ) and online hypothesis generation (p_{gen}) are jointly required to account for children’s behavior: neither component alone reproduces the full distribution of attempts or the rate of correct generalization.

3.2 LLM-PS Results

We evaluated these LLM-based agent variants with three LLM backends, with different architectures and code generation capabilities (GPT-5.2, LOW REASONING, GPT-5.1, DEEPSEEK V3.2). DEEPSEEK V3.2 and GPT-5.1 were instantiated with $n = 10$ particles, as a sufficient number at which the task could be consistently completed in under 70 attempts – the maximal number in

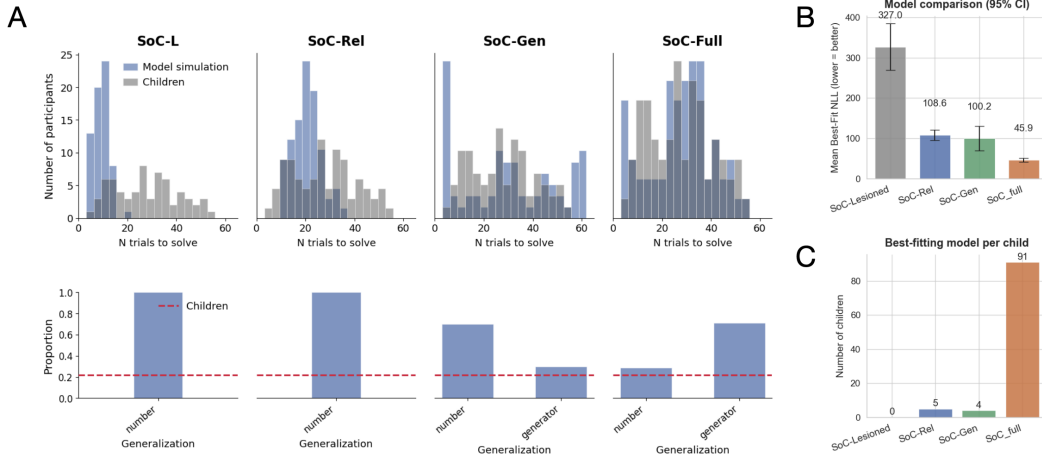


Figure 2: A, Top row. Histograms showing the number of trials required to open all boxes for children and models. Each column represents a different model variant. Bottom row: Distribution of most likely hypotheses for each model after opening all boxes. The correct rule, "number", was generalized to by 22% of children. B. Number of children best fitted by each model. C. Negative Log-likelihoods of each model (shorter = better fit). Error bars indicate 95% CI computed via standard error of the mean across children.

behavioral data. A more capable model, GPT-5.2 was able to complete the task with a single particle. In the single-particle limit, LLM-PS reduces to sequential hypothesis revision: the agent returns a single hypothesis, used by the inference engine to greedily select actions; the rejuvenation step prompts to update this hypothesis given history. Empirically, this simplification is consistent with the view that capable inference systems can operate effectively under a single-hypothesis regime [6, 3].

Figure 3 shows number of actions required to complete the task across agents and LLM backends. The ReAct baselines (not plotted) consistently completed the task in under 15 attempts across backends, confirming that under reliable and fully observable conditions task completion does not require explicit hypothesis maintenance. Notably, ReAct does not generate an executable hypothesis and therefore cannot generalize, demonstrating the necessity of explicit hypothesis representations. Given that DEEPSEEK V3.2 failed to discover the true rule under full observability (LLM-PS-S), it was not evaluated under LLM-PS-P as this would require a larger particle count to achieve task completion, and increase API cost with limited additional diagnostic value.

LLM-PS generates interpretable hypotheses and replicates human performance patterns. Figure 4 shows example trajectories for two model variants using GPT-5.2. Both start with a color-matching hypothesis, consistent with the misleading instruction, but subsequently converge on the correct rule. Like children and SoC models, LLM agents dissociate task completion and generalization under increasing uncertainty. When the model fails to discover the correct rule despite completing the task, the failure modes were similar across LLMs. In such cases, task success was achieved by accumulating coincidental successful box openings driven by approximate hypotheses that combine disparate causes rather than express new unified rules (Appendix B). This property was also captured by the online generator in the SoC. Notably, generalization requires sufficient backend capability, as even under fully observable conditions the weaker models DEEPSEEK V3.2 consistently failed to discover the true rule. Together, these results suggest that given equivalent conditions, LLM-based agents and children express similar performance trends, which can be predicted by operating over a hypothesis space admitting approximate, combinatorial solutions.

Differences between children and LLM-based agents. In addition to these convergent patterns, we find key differences between children’s and LLM behavior. First, LLM-based agents strictly comply with instructions, consistently generating the color-matching hypothesis on the first trial. In contrast, 21 out of 100 children begin by testing a key-box combination that do not match in color, suggesting that children may have competing inductive biases and assume a broader prior in the hypothesis space, or that children may simply be less inclined toward instruction-following compared to LLMs.

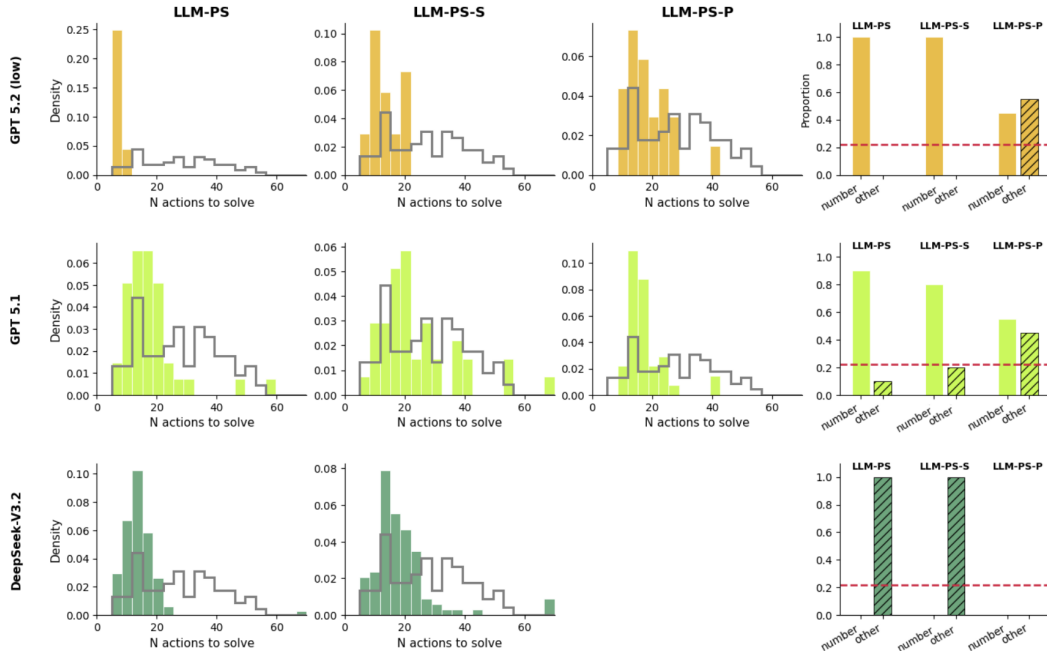


Figure 3: Left: Densities of number of attempts required to open all five boxes under each LLM-PS variant, across LLM backends (rows). Columns correspond to model variants. Right: Generalization of the true rule by each model variant. The red dotted line shows children’s generalization from [30]. Children generalized the true rule 22% of the time upon successful task completion.

Further, LLM-PS-P agents over-observe relative to children (Appendix Figure 5). Children vary substantially in how often and when they seek additional information: 30 out of 100 did not observe any boxes; the majority (79 out of 100) examined only a subset of boxes; 22 out of 100 began the experiment by observing boxes rather than attempting keys. In contrast, LLM-PS-P agents consistently begin interacting with the environment using ATTEMPT actions, switch to systematic observation after a few failed opening attempts, and typically examine all boxes before resuming ATTEMPT actions (Appendix B.4). This difference suggests that children implicitly trade off the informational value of observation against some cost — social or cognitive — that is absent in the LLM setting.

4 Related Work

Bayesian models of learning. Bayesian inference has been widely applied to models of human causal learning [16, 22], including models of structured hypothesis spaces [32, 21] and children’s approximate inference under uncertainty [4, 14]. Most directly related, the Sampling Hypothesis proposes that children sample causal hypotheses from a fully predefined proposal distribution weighted by posterior probability [11, 3, 37]. Our SoC model extends this principle to complex domains where evidence is unreliable and the proposal cannot be entirely predefined. Bramley and Xu [5] find that children generate more diverse hypotheses but converge on correct rules less reliably than adults, a pattern consistent with our finding that children’s hypothesis space admits approximate solutions that succeed at task completion without capturing the true rule.

Program synthesis for inductive reasoning. Much work across AI and cognitive science uses program synthesis to model inductive reasoning. Classically such models have had relatively narrow success because they use custom domain-specific programming languages [17, 2, 13, 22, 26, 7, 18], although many of those successes have been practically and scientifically valuable. Recent work with general-purpose languages such as Python using LLMs has increased the scope of applications [28, 9, 38, 29, 23]. Most closely related, Piriyaikulij et al. [27] also combines SMC-S and Bayesian Experiment Design with LLM-based proposal distributions. Our work differs in core ways, but most

LLM-PS-S (Unreliable evidence)

LLM-PS-P (Partial Obs., Unreliable)

Trial 1: Color rule (misleading prior)

```
def predict(key, box) -> bool:
    # Match key color to box color
    return key.color == box.color
```

Trial 1: Color rule (misleading prior)

```
def predict(key, box) -> bool:
    # Match key color to box color
    return key.color == box.color
```

Trial 6: Partial revision

```
def predict(key, box) -> bool:
    # color for first box, then shape
    if box.position == 1:
        return key.color == box.color
    return (key.shape is not None and
            key.shape == box.shape)
```

Trial 9: Uncertain number belief

```
def predict(key, box) -> bool:
    if key.number is None:
        return False
    if len(box.number) == 0:
        return True # no info: try it
    return key.number in box.number
```

Trial 14: True rule

```
def predict(key, box) -> bool:
    # Key number must match the number
    # of shapes on the box.
    return (key.number is not None and
            key.number in box.number)
```

Trial 18: True rule

```
def predict(key, box) -> bool:
    # Key number must match the number
    # of shapes on the box.
    return (key.number is not None and
            key.number in box.number)
```

Figure 4: Representative hypothesis trajectories generated by LLM-PS-S (left) and LLM-PS-P (right).

importantly in its comparison to children and SoC-models, and in its treatment of partial observability. Notably, our finding that GPT-5.2 completes the task with a single particle is consistent with the view that capable inference systems can operate effectively under a single-hypothesis regime [6]. Our view is that programs induced from naturalistic data cannot assume full observability, and that decision-making must consider uncertainty about both the program hypothesis and the underlying state: Indeed, absent this modeling choice, we cannot explain the human data we consider.

5 Discussion

We introduced a controlled framework for evaluating and comparing inductive inference under uncertainty in human and LLM-based agents. The framework characterizes inference as the interaction between hypothesis generation, noisy evidence under partial observability, and sequential belief revision. While we focus on developing a principled approach to isolating the underlying computational principles within a single domain, our approach instantiates a broad class of problems that deal with latent rule inference. We implement this framework in two complementary ways: the SoC model extending the Sampling Hypothesis [11] to uncertain domains with unbounded hypothesis spaces, and a program synthesis implementation that enables tractable inference over expressive, interpretable, and executable hypotheses.

Using SoC lesion analysis we show that evidence uncertainty and online generation of approximate hypotheses jointly account for children’s behavior. Additional LLM-based agent modeling suggests that, relative to LLM-based agents, children’s inference is shaped by implicit observation costs and operates over a broader prior in the hypothesis space. Notably, the dissociation between task completion and correct generalization observed in children can be replicated in both LLM-based and SoC agents — by generating hypotheses that integrate disparate causes rather than propose new unified rules. We show that such approximate hypotheses can be instrumental both to completing the task without correct generalization, and to accumulating evidence, which can then inform generation of improved unified rules. The extent to which children’s approximate hypothesis generation may follow a similar pattern from cause aggregation to unification remains to be tested in future work.

Our results reveal that LLM-based agents handle unreliable evidence gracefully, and appear to work with a more restrictive prior over hypotheses compared to children. One possible explanation is that training on natural language descriptions of experiment-like tasks induces a bias that such tasks involve a small, structured hypothesis space with a limited set of canonical rules. Further, the models may have been exposed to training on noisy data (i.e. unreliable witnesses) leading to discounting

conflicting evidence. Future work could further examine these interpretations by applying the SoC framework to estimate LLM-based agents’ implicit subjective reliability (ρ) and rule priors (e.g., p_t), comparing these quantities to those inferred from human behavior.

Limitations and Future work Our LLM-PS implementation makes a simplifying assumption that `OBSERVE(i)` actions are fully informative, revealing exact box counts, whereas human observations may only partially reduce uncertainty. This difference may contribute to the more systematic information-seeking behavior observed in LLM-based agents, and could be addressed by introducing graded or noisy observations in future work. Further, our interpretation of LLM behavior remains indirect, as we do not test whether LLM-based agents maintain explicit hypothesis representations or perform likelihood-based updates, as opposed to retrieval. Combining our framework with mechanistic interpretability methods in open-weight models offers a promising direction for distinguishing between these possibilities. To complement current behavioral data, the comparison between human and artificial agents could be further developed through follow-up experiments subjecting human adults and children to identically matched environments (including reliable evidence and fully observable conditions). A further limitation concerns potential data contamination: as the Box Task originates from a published study [30], LLM training corpora may include the task design or solutions. However, agents consistently begin with the misleading hypothesis rather than the true rule, suggesting direct retrieval is unlikely.

Author Contributions

M.K.: Conceptualization, Methodology, Formal Analysis, Visualization, Writing – Original Draft, Review & Editing Project Administration, Funding Acquisition, Supervision. **J.Q.:** Software (Model implementation), Investigation, Visualization. **T.P.** Methodology, Formal Analysis, Writing – Review & Editing. **Z.G.:** Investigation. **M.R.:** Data Curation, Writing – Review. **K.E.:** Writing – Review & Editing. **J.S.:** Writing – Review.

6 Acknowledgments

M. K. was supported by NSERC Discovery grant RGPIN-04045-25. K. E. and W. T. P. supported by an NSF CAREER award.

References

- [1] Kelsey Allen, Franziska Brändle, Matthew Botvinick, Judith E Fan, Samuel J Gershman, Alison Gopnik, Thomas L Griffiths, Joshua K Hartshorne, Tobias U Hauser, Mark K Ho, et al. Using games to understand the mind. *Nature human behaviour*, 8(6):1035–1043, 2024.
- [2] Matej Balog, Alexander L Gaunt, Marc Brockschmidt, Sebastian Nowozin, and Daniel Tarlow. Deepcoder: Learning to write programs. *arXiv preprint arXiv:1611.01989*, 2016.
- [3] Elizabeth Bonawitz, Stephanie Denison, Alison Gopnik, and Thomas L Griffiths. Win-stay, lose-sample: A simple sequential algorithm for approximating bayesian inference. *Cognitive psychology*, 74:35–65, 2014.
- [4] Elizabeth Bonawitz, Stephanie Denison, Thomas L Griffiths, and Alison Gopnik. Probabilistic models, learning algorithms, and response variability: sampling in cognitive development. *Trends in cognitive sciences*, 18(10):497–500, 2014.
- [5] Neil R Bramley and Fei Xu. Active inductive inference in children and adults: A constructivist perspective. *Cognition*, 238:105471, 2023.
- [6] Neil R Bramley, Peter Dayan, Thomas L Griffiths, and David A Lagnado. Formalizing neurath’s ship: Approximate algorithms for online causal learning. *Psychological review*, 124(3):301, 2017.
- [7] François Chollet. On the measure of intelligence. *CoRR*, abs/1911.01547, 2019. URL <http://arxiv.org/abs/1911.01547>.
- [8] Katherine M Collins, Ilija Sucholutsky, Umang Bhatt, Kartik Chandra, Lionel Wong, Mina Lee, Cedegao E Zhang, Tan Zhi-Xuan, Mark Ho, Vikash Mansinghka, et al. Building machines that learn and think with people. *Nature human behaviour*, 8(10):1851–1863, 2024.

- [9] Nicola Dainese, Matteo Merler, Minttu Alakuijala, and Pekka Marttinen. Generating code world models with large language models guided by monte carlo tree search. In *The Thirty-eighth Annual Conference on Neural Information Processing Systems*, 2024. URL <https://arxiv.org/abs/2405.15383>.
- [10] Pierre Del Moral, Arnaud Doucet, and Ajay Jasra. Sequential monte carlo samplers. *Journal of the Royal Statistical Society Series B: Statistical Methodology*, 68(3):411–436, 05 2006. ISSN 1369-7412. doi: 10.1111/j.1467-9868.2006.00553.x. URL <https://doi.org/10.1111/j.1467-9868.2006.00553.x>.
- [11] Stephanie Denison, Elizabeth Bonawitz, Alison Gopnik, and Thomas L Griffiths. Rational variability in children’s causal inferences: The sampling hypothesis. *Cognition*, 126(2):285–300, 2013.
- [12] Michael C Frank. Openly accessible llms can help us to understand human cognition. *Nature Human Behaviour*, 7(11):1825–1827, 2023.
- [13] Noah D Goodman, Joshua B Tenenbaum, Jacob Feldman, and Thomas L Griffiths. A rational analysis of rule-based concept learning. *Cognitive science*, 32(1):108–154, 2008.
- [14] Alison Gopnik. Childhood as a solution to explore–exploit tensions. *Philosophical Transactions of the Royal Society B*, 375(1803):20190502, 2020.
- [15] Alison Gopnik, Clark Glymour, David M Sobel, Laura E Schulz, Tamar Kushnir, and David Danks. A theory of causal learning in children: causal maps and bayes nets. *Psychological review*, 111(1):3, 2004.
- [16] Thomas L Griffiths, Joshua B Tenenbaum, and Charles Kemp. Bayesian inference. *The Oxford handbook of thinking and reasoning*, pages 22–35, 2012.
- [17] Sumit Gulwani. Automating string processing in spreadsheets using input-output examples. *SIGPLAN Not.*, 46(1):317–330, January 2011. ISSN 0362-1340. doi: 10.1145/1925844.1926423. URL <https://doi.org/10.1145/1925844.1926423>.
- [18] Sumit Gulwani, José Hernández-Orallo, Emanuel Kitzelmann, Stephen H. Muggleton, Ute Schmid, and Benjamin Zorn. Inductive programming meets the real world. *Commun. ACM*, 58(11):90–99, October 2015. ISSN 0001-0782. doi: 10.1145/2736282. URL <https://doi.org/10.1145/2736282>.
- [19] Philip Nicholas Johnson-Laird. *Mental models: Towards a cognitive science of language, inference, and consciousness*. Number 6. Harvard University Press, 1983.
- [20] Leslie Pack Kaelbling, Michael L. Littman, and Anthony R. Cassandra. Planning and acting in partially observable stochastic domains. *Artificial Intelligence*, 101(1-2):99–134, 1998.
- [21] Charles Kemp and Joshua B Tenenbaum. Structured statistical models of inductive reasoning. *Psychological review*, 116(1):20, 2009.
- [22] Brenden M Lake, Ruslan Salakhutdinov, and Joshua B Tenenbaum. Human-level concept learning through probabilistic program induction. *Science*, 350(6266):1332–1338, 2015.
- [23] Wen-Ding Li and Kevin Ellis. Is programming by example solved by llms? In *Proceedings of the 38th International Conference on Neural Information Processing Systems*, NIPS ’24, Red Hook, NY, USA, 2024. Curran Associates Inc. ISBN 9798331314385.
- [24] Dennis V Lindley. On a measure of the information provided by an experiment. *The Annals of Mathematical Statistics*, 27(4):986–1005, 1956.
- [25] David Marr. *Vision: A Computational Investigation into the Human Representation and Processing of Visual Information*. W. H. Freeman, 1982.
- [26] Steven Thomas Piantadosi. *Learning and the language of thought*. PhD thesis, MIT, 2011.
- [27] Top Piriyakulkij, Cassidy Langenfeld, Tuan Anh Le, and Kevin Ellis. Doing experiments and revising rules with natural language and probabilistic reasoning. *Advances in Neural Information Processing Systems*, 37:53102–53137, 2024.
- [28] Wasu Top Piriyakulkij, Yichao Liang, Hao Tang, Adrian Weller, Marta Kryven, and Kevin Ellis. Poe-world: Compositional world modeling with products of programmatic experts. *Advances in Neural Information Processing Systems (NeurIPS)*, 2025.
- [29] Linlu Qiu, Liwei Jiang, Ximing Lu, Melanie Sclar, Valentina Pyatkin, Chandra Bhagavatula, Bailin Wang, Yoon Kim, Yejin Choi, Nouha Dziri, and Xiang Ren. Phenomenal yet puzzling: Testing inductive reasoning capabilities of language models with hypothesis refinement. In *The Twelfth International Conference on Learning Representations*, 2024. URL <https://openreview.net/forum?id=bMt7oaj12a>.

- [30] Mia Radovanovic, Ece Yucer, and Jessica A Sommerville. Girls persist more but divest less from ineffective teaching than boys. *Journal of Experimental Psychology: General*, 2024.
- [31] Tom Rainforth, Adam Foster, Desi R Ivanova, and Freddie Bickford Smith. Modern bayesian experimental design. *Statistical Science*, 39(1):100–114, 2024.
- [32] Joshua Stewart Rule. *The child as hacker: building more human-like models of learning*. PhD thesis, Massachusetts Institute of Technology, 2020.
- [33] Herbert A Simon. A behavioral model of rational choice. *The quarterly journal of economics*, pages 99–118, 1955.
- [34] Christopher Summerfield. *Natural General Intelligence: How understanding the brain can help us build AI*. Oxford University Press, 2023.
- [35] Hao Tang, Darren Key, and Kevin Ellis. Worldcoder, a model-based llm agent: Building world models by writing code and interacting with the environment. *Advances in Neural Information Processing Systems*, 37:70148–70212, 2024.
- [36] Bas van Opheusden and Wei Ji Ma. Tasks for aligning human and machine planning. *Current Opinion in Behavioral Sciences*, 29:127–133, 2019.
- [37] Edward Vul, Noah Goodman, Thomas L Griffiths, and Joshua B Tenenbaum. One and done? optimal decisions from very few samples. *Cognitive science*, 38(4):599–637, 2014.
- [38] Ruo Cheng Wang, Eric Zelikman, Gabriel Poesia, Yewen Pu, Nick Haber, and Noah Goodman. Hypothesis search: Inductive reasoning with language models. In *The Twelfth International Conference on Learning Representations*, 2024. URL <https://openreview.net/forum?id=G7UtIGQmjm>.
- [39] Shunyu Yao, Jeffrey Zhao, Dian Yu, Nan Du, Irina Shafran, Karthik Narasimhan, and Yuan Cao. ReAct: Synergizing reasoning and acting in language models. In *International Conference on Learning Representations*, 2023.
- [40] Lance Ying, Katherine M Collins, Prafull Sharma, Cedric Colas, Kaiya Ivy Zhao, Adrian Weller, Zenna Tavares, Phillip Isola, Samuel J Gershman, Jacob D Andreas, et al. Assessing adaptive world models in machines with novel games. URL <https://arxiv.org/abs/2507.12821>, 2025.

A The Box Task Setup

The Box Task environment is introduced in [30]. Below we summarize relevant details.

Children completed the experiment in person, in four phases:

1. *Practice*: Participants tried plain keys on a plain practice box to familiarize themselves with the key action, including both correct and incorrect keys.
2. *Instruction*: Children viewed an instructional video in which a teacher demonstrated an incorrect color-matching rule, using a red-fobbed key to open the red box. This demonstration was confounded: for the red box only, the correct key happened to match both color and number. For all other boxes, color-matched keys were incorrect. The teacher communicated the rule as definitive and provided no indication that it would fail.
3. *Test*: The five boxes were arranged in a fixed order in front of the participant. All 13 keys were placed in a single pile. Children were instructed to open all five boxes within a 5-minute time limit, working independently. The experimenter remained present but provided no feedback. Boxes could be picked up and examined. The test ended upon opening all five boxes or at time expiry.
4. *Generalization*: Four forced-choice trials using novel box images were presented on a tablet screen. For each box, four keys were presented: a color-matched key, a shape-matched key, a number-matched key (correct), and a number foil. Children selected which key they believed would open the box.

Box Task Environment. The boxes were uniquely colored physical objects, 11cm x 11.9cm x 10.6cm, featuring a different number of shapes on its faces. Each shape was labeled with a number to indicate quantity (e.g., the pink box had two clouds, labeled "1" and "2"). Each box had at least one shape. Keys were metal physical objects. Each key had a colored tag displaying either a number or a shape.

Partial Observability. The task is partially observable: subjects initially observe each box’s color and shape identity, but not the total number of shape instances. The exact shape count is revealed only if the subject picks up and examines the box.

At each time t , subjects choose between:

- **Observe:** $\text{observe}(i)$ reveals the exact number of shapes on box i
- **Attempt:** $\text{attempt}(i, j)$ attempts to open box i with key j , where $i \in \{1, \dots, 5\}$ and $j \in \{1, \dots, 13\}$

Box	Order	color	Shape	Shape count (Number)
B1	1	red	moon	?
B2	2	pink	cloud	?
B3	3	white	diamond	?
B4	4	purple	heart	?
B5	5	blue	triangle	?

Table 1: Initial box configuration as observed by subjects. color, shape identity, and order are fully observable. Shape count requires picking up the box.

Key	color	Shape	Number
red1	red		1
pink6	pink		6
grey2	grey		2
greycloud	grey	cloud	
orange4	orange		4
green3	green		3
bluestar	blue	star	
yellow5	yellow		5
greenheart	green	heart	
white7	white		7
triangleyellow	yellow	triangle	
diamondorange	orange	diamond	
purplearrow	purple	arrow	

Table 2: Set of available keys. Each key is associated with a color and either a number or a shape (but not both). Numbers range beyond the possible box counts, introducing distractors; shape-based keys provide alternative matching cues.

Box	Order	color	Shape	Number
B1	1	red	moon	1
B2	2	pink	cloud	2
B3	3	white	diamond	4
B4	4	purple	heart	3
B5	5	blue	triangle	5

Table 3: True (unobserved) configuration of the boxes. The true number of shapes on each box becomes observable with inspection.

B LLM Prompts and Output Examples

B.1 LLM-PS-P (unreliable evidence, partially observable)

System Prompt

You are an intelligent agent playing a game.
Your task is to open 5 boxes using 13 keys in fewest attempts.
You do not need special skills to play this game.
This game can be played by an 8-12 year old child.

User Prompt

For each box there is a key that opens it.
The goal of the game is to find the right key for each box, using as few actions as possible.
You have a demonstration video from a teacher telling you how to open all boxes.
In the video, the teacher says:
"I'm going to show you the right way to unlock the boxes.
To open the boxes, you have to use a key that matches the color of the box.
So, to open this red box, I'm going to use this red key.
Great, now you can open all the doors!"

Each key has an identifier (id) and a color.
Each key also has either a number or a shape, but not both.

Each box has a color. It also has a shape, which is printed on at least one of its faces.
Not all faces are visible to you initially, but the game allows you to pick up boxes and examine them to get more information.

Here are the boxes, lined up in this order:
The first box is red, has a moon shape.
The second box is pink, has a cloud shape.
The third box is white, has a diamond shape.
The fourth box is purple, has a heart shape.
The fifth box is blue, has a triangle shape.

Here are the 13 keys (in no specific order):
The red key is red and has the number 1.
The pink key is pink and has the number 6.
The grey2 key is grey and has the number 2.
The cloud key is grey and has a cloud shape.
The orange4 key is orange and has the number 4.
The green3 key is green and has the number 3.
The blue key is blue and has a star shape.
The yellow5 key is yellow and has the number 5.
The heart key is green and has a heart shape.
The white key is white and has the number 7.
The triangle key is yellow and has a triangle shape.
The diamond key is orange and has a diamond shape.
The purple key is purple and has an arrow shape.

You can interact with this environment by taking two types of actions:
(1) Attempt Action: write Python code that will be used to generate opening attempts, or
(2) Observe Action: request more information about a given box.

To Take the Observe Action, your output should be exactly
"PICK UP x", where x is the box id (do not use any other attributes of the box)

To take an Attempt Action, you will need to write a Python function that specifies a hypothesis about which keys open which boxes.

Your output should use the given starter code, and complete the function called predict according to its signature.
Your output should contain only the Python program for predict, absolutely nothing else. It should NOT contain the Key or Box classes.

Here is the history of actions taken and observed evidence.
Please use them to make your decision:

```
Open box {BOX1} with key {KEY1}: {OUTCOME1}
Examine {BOX2}: {BOX2.number (real)} faces have shapes on them
Open box {BOX3} with key {KEY3}: {OUTCOME3}
...
```

Here is the starter code for attempt action

```
def predict(key, box) -> bool:
    # key is a Key object
    # box is a Box object
    # fill in your code

class Key:
    def __init__(self, id: str, color: str, number: Optional[int], shape: Optional[str]):
        self.id = id
        self.color = color
        self.number = number
        self.shape = shape

class Box:
    def __init__(self, id: str, color: str, shape: str, number: set, position: int):
        self.id = id
        self.color = color
        self.shape = shape
        self.position = position
        self.number: set
        # Current belief over number of shapes on this box.
        # Unknown until PICK UP action is taken.
        # After PICK UP: collapses to a singleton set containing the exact value.
        # In predict(), handle both uncertain and certain cases.
```

Here are the accurate data for all keys and boxes.
The indexing of the arrays correspond to the line-up order of boxes and keys.

```
key_data = {
    "id": ["red", "pink", "grey2", "cloud", "orange4", "green3", "blue", "yellow5",
           "heart", "white", "triangle", "diamond", "purple"],
    "color": ["red", "pink", "grey", "grey", "orange", "green", "blue", "yellow",
              "green", "white", "yellow", "orange", "purple"],
    "number": [1, 6, 2, None, 4, 3, None, 5, None, 7, None, None, None],
    "shape": [None, None, None, "cloud", None, None, "star", None, "heart", None,
              "triangle", "diamond", "arrow"]
}

box_data = {
    "id": ["red", "pink", "white", "purple", "blue"],
    "color": ["red", "pink", "white", "purple", "blue"],
    "shape": ["moon", "cloud", "diamond", "heart", "triangle"],
    "number": [set(), set(), set(), set(), set()],
    "position": [1, 2, 3, 4, 5],
}
```

Now is your turn. Respond with either Observe or Attempt action.

Example of partially correct Final Hypothesis GPT-5.2, LLM-PS-P

Here the agent fails to observe all boxes, and instead produces a lazy hypothesis that uses the correct rule, but only for boxes that it observed.

```
def predict(key, box) -> bool:
    if key.number is not None:
        if hasattr(box, "number") and isinstance(box.number, set) and len(box.number) > 0:
            return key.number in box.number
        # match by color when number evidence isn't available.
    return key.color == box.color
```

B.2 LLM-PS-S (unreliable evidence, fully observable)

System Prompt

You are an intelligent agent playing a game.
Your task is to open 5 boxes using 13 keys in fewest attempts.
You do not need special skills to play this game.
This game can be played by an 8-12 year old child.

User Prompt: Context

For each box there is a key that opens it.
The goal of the game is to find the right key for each box.
You have a demonstration video from a teacher telling you how to open all boxes.
In the video, the teacher says:
"I'm going to show you the right way to unlock the boxes.
To open the boxes, you have to use a key that matches the color of the box.
So, to open this red box, I'm going to use this red key.
Great, now you can open all the doors!"

The red box has 1 moon shape.
The pink box has 2 cloud shapes. Each cloud is numbered from 1 to 2.
The white box has 4 diamond shapes. Each diamond is numbered from 1 to 4.
The purple box has 3 heart shapes. Each heart is numbered from 1 to 3.
The blue box has 5 triangle shapes. Each triangle is numbered from 1 to 5.

Here are the 13 keys (in no specific order):
The red key is red and has the number 1.
The pink key is pink and has the number 6.
The grey2 key is grey and has the number 2.
The cloud key is grey and has a cloud shape.
The orange4 key is orange and has the number 4.
The green3 key is green and has the number 3.
The blue key is blue and has a star shape.
The yellow5 key is yellow and has the number 5.
The heart key is green and has a heart shape.
The white key is white and has the number 7.
The triangle key is yellow and has a triangle shape.
The diamond key is orange and has a diamond shape.
The purple key is purple and has an arrow shape.

Here is the accurate code data for all keys and boxes in the environment.
The number attribute of boxes denotes the number of faces with a shape on them.

```
key_data = {
```

```

    "id": ["red", "pink", "grey2", "cloud", "orange4", "green3", "blue",
          "yellow5", "heart", "white", "triangle", "diamond", "purple"],
    "color": ["red", "pink", "grey", "grey", "orange", "green", "blue",
             "yellow", "green", "white", "yellow", "orange", "purple"],
    "number": [1, 6, 2, None, 4, 3, None, 5, None, 7, None, None, None],
    "shape": [None, None, None, "cloud", None, None, "star", None, "heart",
             None, "triangle", "diamond", "arrow"]
}

box_data = {
    "id": ["red", "pink", "white", "purple", "blue"],
    "color": ["red", "pink", "white", "purple", "blue"],
    "shape": ["moon", "cloud", "diamond", "heart", "triangle"],
    "number": [1, 2, 4, 3, 5],
    "position": [1, 2, 3, 4, 5],
}

```

A hypothesis is a valid Python program that can be executed to predict the outcome of a given key and box.

The Python program should have the following signature:

```

def predict(key, box) -> bool:
    # key is a Key object
    # box is a Box object
    # fill in your code

```

The Key and Box objects are defined as follows.
The default value for optional parameters is None.

```

class Key:
    def __init__(self, id: str, color: str, number: Optional[int], shape: Optional[str]):
        self.id = id
        self.color = color
        self.number = number
        self.shape = shape

class Box:
    def __init__(self, id: str, color: str, number: int, shape: str):
        self.id = id
        self.color = color
        self.number = number
        self.shape = shape

```

User Prompt: Generate Hypothesis

Now, it is your turn to generate a hypothesis.
Your hypothesis should be a Python program that contains exactly the predict function.
Include the signature exactly as provided, no type hints for argument.

Your output should contain only the Python program, absolutely nothing else.
Your output should NOT contain the Key or Box classes.

User Prompt: Refine Hypothesis

Now, your task is to improve and refine an existing hypothesis that performs poorly on existing evidence.

This is the hypothesis: {HYPOTHESIS},

Here is the evidence from previous attempts.

Remember that the keys and boxes are physical objects, so for some probability the correct key might fail to open the correct box due to a mechanical failure.

```
Open box {BOX1} with key {KEY1}: {OUTCOME1}
Open box {BOX2} with key {KEY2}: {OUTCOME2}
...
```

Generate a new hypothesis.

Your hypothesis should be a Python program that contains exactly the predict function, including the provided signature.

Your output should contain only the Python program, absolutely nothing else.

Your output should NOT contain the Key or Box classes.

Example of Partially Correct Final Hypothesis, GPT-5.2, LLM-PS-S

The agent never forgets the misleading rule, but still successfully completes the task once the true rule has been introduced as part of the hypotheses.

```
def predict(key, box) -> bool:
    if key.number is not None:
        return key.number == box.number
    return key.color == box.color
```

Examples of Incorrect Final Hypotheses: DEEPSEEK V3.2, LLM PS-S

```
def predict(key, box) -> bool:
    if key.shape is not None and key.shape == box.shape:
        return True
    if key.number is not None and key.number == box.number:
        return True
    return False
```

```
def predict(key, box) -> bool:
    if key.shape is not None:
        if key.shape == "cloud" and box.shape == "cloud":
            return True
        if key.shape == "heart" and box.shape == "heart":
            return True
        if key.shape == "triangle" and box.shape == "triangle":
            return True
        if key.shape == "diamond" and box.shape == "diamond":
            return True
        if key.shape == "star" and box.shape == "moon":
            return False
        if key.shape == "arrow" and box.shape == "moon":
            return False
    if key.number is not None:
        if key.number == box.number:
            return True
    return False
```

B.3 LLM-PS (reliable evidence, fully observable)

System Prompt

You are an intelligent agent playing a game.
Your task is to open 5 boxes using 13 keys in fewest attempts.
You do not need special skills to play this game.
This game can be played by an 8-12 year old child.

User Prompt: Context

For each box there is a key that opens it.
The goal of the game is to find the right key for each box.
You have a demonstration video from a teacher telling you how to open all boxes.
In the video, the teacher says:
"I'm going to show you the right way to unlock the boxes.
To open the boxes, you have to use a key that matches the color of the box.
So, to open this red box, I'm going to use this red key.
Great, now you can open all the doors!"

The red box has 1 moon shape.
The pink box has 2 cloud shapes. Each cloud is numbered from 1 to 2.
The white box has 4 diamond shapes. Each diamond is numbered from 1 to 4.
The purple box has 3 heart shapes. Each heart is numbered from 1 to 3.
The blue box has 5 triangle shapes. Each triangle is numbered from 1 to 5.

Here are the 13 keys (in no specific order):
The red key is red and has the number 1.
The pink key is pink and has the number 6.
The grey2 key is grey and has the number 2.
The cloud key is grey and has a cloud shape.
The orange4 key is orange and has the number 4.
The green3 key is green and has the number 3.
The blue key is blue and has a star shape.
The yellow5 key is yellow and has the number 5.
The heart key is green and has a heart shape.
The white key is white and has the number 7.
The triangle key is yellow and has a triangle shape.
The diamond key is orange and has a diamond shape.
The purple key is purple and has an arrow shape.

Here is the accurate code data for all keys and boxes in the environment.
The number attribute of boxes denotes the number of faces with a shape on them.

```
key_data = {
    "id": ["red", "pink", "grey2", "cloud", "orange4", "green3", "blue",
          "yellow5", "heart", "white", "triangle", "diamond", "purple"],
    "color": ["red", "pink", "grey", "grey", "orange", "green", "blue",
             "yellow", "green", "white", "yellow", "orange", "purple"],
    "number": [1, 6, 2, None, 4, 3, None, 5, None, 7, None, None, None],
    "shape": [None, None, None, "cloud", None, None, "star", None, "heart",
             None, "triangle", "diamond", "arrow"]
}

box_data = {
    "id": ["red", "pink", "white", "purple", "blue"],
    "color": ["red", "pink", "white", "purple", "blue"],
    "shape": ["moon", "cloud", "diamond", "heart", "triangle"],
    "number": [1, 2, 4, 3, 5],
    "position": [1, 2, 3, 4, 5],
}
```

A hypothesis is a valid Python program that can be executed
to predict the outcome of a given key and box.
The Python program should have the following signature:

```
def predict(key, box) -> bool:
```

```
# key is a Key object
# box is a Box object
# fill in your code
```

The Key and Box objects are defined as follows.
The default value for optional parameters is None.

```
class Key:
    def __init__(self, id: str, color: str, number: Optional[int], shape: Optional[str]):
        self.id = id
        self.color = color
        self.number = number
        self.shape = shape
class Box:
    def __init__(self, id: str, color: str, number: int, shape: str):
        self.id = id
        self.color = color
        self.number = number
        self.shape = shape
```

User Prompt: Generate Hypothesis

Now, it is your turn to generate a hypothesis.
Your hypothesis should be a Python program that contains exactly the predict function.
Include the signature exactly as provided, no type hints for argument.

Your output should contain only the Python program, absolutely nothing else.
Your output should NOT contain the Key or Box classes.

User Prompt: Refine Hypothesis

Now, your task is to improve and refine an existing hypothesis that performs poorly on existing evidence.

This is the hypothesis: {HYPOTHESIS},

Here are the evidence from previous attempts.

```
Open box {BOX1} with key {KEY1}: {OUTCOME1}
Open box {BOX2} with key {KEY2}: {OUTCOME2}
...
```

Generate a new hypothesis.
Your hypothesis should be a Python program that contains exactly the predict function, including the provided signature.
Your output should contain only the Python program, absolutely nothing else.
Your output should NOT contain the Key or Box classes.

Example of Incorrect Final Hypothesis (both GPT-5.2 and DEEPSEEK V3.2)

```
def predict(key, box) -> bool:
    # Primary rule supported by evidence: numbered keys open boxes with matching counts
    if key.number is not None:
        return key.number == box.number

    # If no number, try matching the depicted shape
    if key.shape is not None:
        return key.shape == box.shape
```

```
# Fallback: match color (as suggested by the demonstration)
return key.color == box.color
```

B.4 ReAct (fully observable)

System Prompt

You are an intelligent agent playing a game.
Your task is to open 5 boxes using 13 keys in fewest attempts.
You do not need special skills to play this game.
This game can be played by an 8-12 year old child.

User Prompt

For each box there is a key that opens it, so the goal of the game is to find the right key for each box.
You have a demonstration video from a teacher telling you how to open all boxes. In the video, the teacher says:
"I'm going to show you the right way to unlock the doors. To open the doors, you have to use a key that matches the color of the box. So, to open this red box, I'm going to use this red key. Great, now you can open all the doors!"

Here are the boxes, lined up in this order:
The red box has 1 moon shape.
The pink box has 2 cloud shapes.
Each cloud is numbered from 1 to 2.
The white box has 4 diamond shapes.
Each diamond is numbered from 1 to 4.
The purple box has 3 heart shapes.
Each heart is numbered from 1 to 3.
The blue box has 5 triangle shapes.
Each triangle is numbered from 1 to 5.

Here are the 13 keys (in no specific order):
The red1 key is red and has the number 1.
The pink6 key is pink and has the number 6.
The grey2 key is grey and has the number 2.
The greycloud key is grey and has a cloud shape.
The orange4 key is orange and has the number 4.
The green3 key is green and has the number 3.
The bluestar key is blue and has a star shape.
The yellow5 key is yellow and has the number 5.
The greenheart key is green and has a heart shape.
The white7 key is white and has the number 7.
The triangleyellow key is yellow and has a triangle shape.
The diamondorange key is orange and has a diamond shape.
The purplearrow key is purple and has an arrow shape.

You have already tried the following keys-box combinations:
[BOX, KEY, OUTCOME]

Now is your turn to open the boxes.
Respond in the format "key, box" (e.g. "red1, red") and do not include any other text in the response.

Example LLM-PS-P Run Log

Below we show the first 11 trials from a representative run log of a single LLM-PS-P episode (GPT-5.2 with low reasoning). The log shows the interleaving of ATTEMPT and OBSERVE actions, and the evolution of hypotheses across trials.

<i>t</i>	Action	Detail
1	Attempt	<pre>def predict(key, box) -> bool: # Open a box if the key color matches the box color. return key.color == box.color</pre> <p><i>Attempt: white → white: failure</i></p>
2	Attempt	<pre>def predict(key, box) -> bool: shape_keys = {'cloud', 'diamond', 'heart', 'triangle'} if box.shape in shape_keys: return (key.shape is not None) and (key.shape == box.shape) # Moon box: fall back to color match return key.color == box.color</pre> <p><i>Attempt: heart → purple: failure</i></p>
3	Observe	PICK UP purple → purple: 3 faces have shape on them.
4	Observe	PICK UP red → red: 1 face has shape on it.
5	Observe	PICK UP white → white: 4 faces have shape on them.
6	Observe	PICK UP pink → pink: 2 faces have shape on them.
7	Attempt	<pre>def predict(key, box) -> bool: # Revert to color matching. return key.color == box.color</pre> <p><i>Attempt: purple → purple: failure</i></p>
8	Observe	PICK UP blue → blue: 5 faces have shape on them.
9	Attempt	<pre>def predict(key, box) -> bool: # Shape counts observed: red=1, pink=2, # purple=3, white=4, blue=5. # Key numbers match shape counts exactly. shape_counts = { 'red': 1, 'pink': 2, 'purple': 3, 'white': 4, 'blue': 5 } return (key.number is not None and key.number == shape_counts.get(box.color))</pre> <p><i>Attempt: grey2 → pink: failure</i></p>
10	Attempt	<pre>def predict(key, box) -> bool: # match key number to number of shapes on the box. return (key.number is not None and key.number in box.number)</pre> <p><i>Attempt: red1 → red: success</i></p>
11	Attempt	<pre>def predict(key, box) -> bool: # match key number to number of shapes on the box. return (key.number is not None and key.number in box.number)</pre> <p><i>Attempt: grey2 → pink: success</i></p>

Outcome: Task solved within 17 trials. 5 boxes opened. correct rule discovered on Trials 9, and 10

Notes. The agent correctly issues OBSERVE actions to resolve partial observability (trials 3–6, 8), accumulating shape counts. Trial 9 shows a failure due to unreliable evidence when testing a *correct* action. This episode illustrates both the information-seeking behavior enabled by OBSERVE actions, and LLMs’ ability to recover from unreliable actions.

Other LLM failure modes

In pilot experiments we also evaluated several LLM backends not included in the present analysis because of poor program synthesis performance (i.e. gpt-4.1, qwen 3.5). Their failure modes were dominated by:

- failure to generate valid executable code
- generating executable code that was not logically valid (i.e. always returns FALSE upon evaluation)

Thus, our modeling framework is limited to LLM backends that have the ability to generate executable code consistently based on prompts.

C Model Fitting

Exact parameter inference of SoC parameters $\theta = (\rho, p_{gen}, p_t)$ at the individual level is intractable for three reasons.

First, the generator in the proposal distribution makes the hypothesis space effectively unbounded. The pre-specified rules are finite and enumerable, but the generator produces novel SoCs not in the pre-defined set. Assuming h_t are all hypotheses that can be sampled from the proposal at step t given history, and θ are model parameters, the marginal likelihood

$$P(e_t | e_{1:t-1}, \theta) = \sum_{h_t} P(e_t | h_t) P(h_t | e_{1:t-1}, \theta)$$

is computationally intractable.

Second, because h_t is sampled from the proposal, two runs of an identically parametrized model can produce qualitatively different hypothesis trajectories. This means the likelihood surface $P(e_{1:T} | \theta)$, estimated by simulation, has high variance — making optimization unreliable. For instance, the marginal likelihood equation cannot be reliably estimated using a few samples with importance weighting (i.e one sample is sometimes used in variational inference) as the variance of the estimator scales with the mismatch between proposal and posterior. Given the generator hypothesis space and long trajectories, this mismatch is large enough that estimates are unreliable in practice.

Third, individual data are sparse. Each participant produces a single trajectory of $T \approx 10\text{--}60$ trials. With one observed trajectory per individual, the marginal likelihood is a noisy estimator of θ : the signal-to-noise ratio is insufficient to recover individual parameters reliably.

This makes exact individual-level parameter recovery ill-posed. We therefore approximate inference using a coarse discrete grid search, selecting the parameter setting that maximises log-likelihood for each child independently. This avoids the intractability of continuous optimisation while preserving sensitivity to individual differences in behavior.

C.1 Model Fitting

Probability tables

For each model variant and parameter setting θ_i , we obtain a pre-computed probability table giving the probability that the model has opened exactly $n \in \{0, 1, 2, 3, 4, 5\}$ boxes by trial $t \in \{1, \dots, 70\}$:

$$P(n | t, \theta_i).$$

These tables were produced by running 100 forward simulations of each model at each parameter setting and recording the empirical frequency of each count n at each trial t .

Child observations

Let $n_{j,t}$ denote the *cumulative* number of distinct boxes opened by child j up to and including trial t . Children completed at most 70 trials.

Log-likelihood

For child j under parameter setting θ_i , the log-likelihood is

$$\log \mathcal{L}(j, \theta_i) = \sum_{t=1}^{T_j} \log \max(P(n_{j,t} | t, \theta_i), \varepsilon),$$

where $T_j \leq 70$ is the number of trials recorded for child j . and $\varepsilon = 0.01 = 1/N$ is a small floor applied before taking the logarithm. Parameter rankings were verified to be stable across alternative grid and smoothing choices.

Parameter selection

For each model variant with free parameters, we select the setting that maximises the log-likelihood for each child independently:

$$\theta_j^* = \arg \max_{\theta_i} \log \mathcal{L}(j, \theta_i).$$

The parameter grids are:

- **SoC-Gen:** $p_{gen} \in \{0.1, 0.2, 0.3, 0.4, 0.5, 0.6, 0.7, 0.8, 0.9\}$ (9 settings; ρ lesioned).
- **SoC-Rel:** $\rho \in \{(1, 1), (1, 2), (1, 3), (2, 1), (3, 1), (4, 1), (5, 1), (6, 1), (9, 1), (15, 1), (19, 1)\}$ (11 settings; p_{gen} lesioned). The tuples represent parameters given for a Beta distribution prior. Note that the subjective reliability parameter ρ is defined in the main text as a scalar in $(0, 1]$, corresponding to the expected value of a Beta(α, β) prior. During fitting, we sweep over (α, β) pairs rather than scalar values directly, with $\mathbb{E}[\rho] = \alpha/(\alpha + \beta)$. The grid $\{(3, 1), (2, 1), (1, 1), \dots, (19, 1)\}$ thus spans $\mathbb{E}[\rho] \in [0.05, 0.95]$.
- **SoC-Full:** all combinations of the above two grids (99 settings).
- **SoC-Lesioned:** no free parameters, both p_{gen}, ρ lesioned.

The prior probability of the true rule p_t is introduced as a free parameter in the main text. In practice, we first swept $p_t \in [0.01, 0.20]$ at 10 levels, and found fitted values to be consistently concentrated near $p_t = 0.02$ across children. We therefore fixed $p_t = 0.02$ for all variants in the grid search reported here, reducing the search space without meaningful impact on model fit. The grids and heatmaps in Figure 12 reflect this fixed value.

The best-fit log-likelihood for child j under a given model variant is $\log \mathcal{L}_j^* = \log \mathcal{L}(j, \theta_j^*)$. For SoC-Lesioned, $\log \mathcal{L}_j^*$ is computed directly at the single fixed parameter setting.

Model comparison

At the population level, we compute the mean best-fit log-likelihood across children for each model variant:

$$\overline{\log \mathcal{L}} = \frac{1}{J} \sum_{j=1}^J \log \mathcal{L}_j^*,$$

with 95% confidence intervals derived from the standard error of the mean ($\pm 1.96 \times \text{SE}$, where $\text{SE} = \hat{\sigma}/\sqrt{J}$ and $\hat{\sigma}$ is the sample standard deviation across children).

To determine which model best explains each child’s behavior, we identify the variant with the highest $\log \mathcal{L}_j^*$ and report the count of children for whom each variant is selected. Pairwise differences in model fit are tested using paired t -tests on $\log \mathcal{L}_j^*$ values (same children scored under each model), with effect sizes reported as Cohen’s d for paired samples:

$$d = \frac{\overline{\Delta}}{\hat{\sigma}_{\Delta}},$$

where $\overline{\Delta}$ and $\hat{\sigma}_{\Delta}$ are the mean and standard deviation of the per-child log-likelihood differences.

Model complexity adjustment

To account for differences in model complexity, we additionally compare models using the Akaike Information Criterion (AIC), computed per child as $AIC_j = 2 \log \mathcal{L}_j^* + 2k$, where k is the number of free parameters (SoC-Lesioned: $k = 0$; SoC-Rel, SoC-Gen: $k = 1$; SoC-Full: $k = 2$). Mean AIC values across children are reported in Table 4.

Model	Mean NLL	k	Mean AIC
SoC-Lesioned	326.96	0	653.92
SoC-Rel	108.61	1	219.22
SoC-Gen	100.20	1	202.40
SoC-Full	45.89	2	95.78

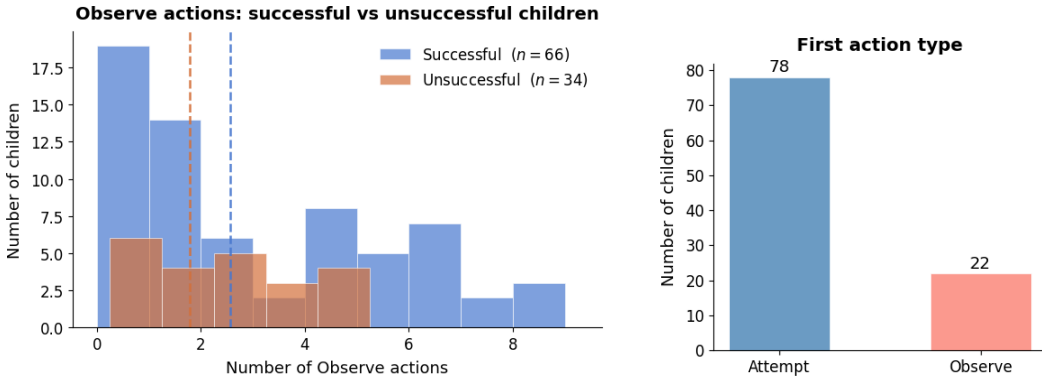
Table 4: Model comparison by mean AIC (lower is better). The complexity penalty for SoC-Full ($2k = 4$) is negligible relative to the NLL differences, confirming that the fit improvement of the full model outweighs its additional free parameters.

D Additional Behavioral Results

Here we show additional analysis of children’s behavior in the Box Task, which motivate our model.

D.1 Observations

An OBSERVE action is defined as picking up a box to examine its hidden faces. Children vary substantially in how often they seek additional information, with many children making no observations at all (Figure 5). Notably, children who successfully completed the task observed boxes more often (Successful: mean 2.56, SD 2.52; Unsuccessful: mean 1.79, SD 1.76). Out of 100, 79 children made fewer than 5 Observe actions, implying that not all boxes were observed. This variability motivates the partial observability condition in LLM-PS-P, and contrasts with LLM-PS-P agents, which observe systematically until all boxes are examined.



(a) Distribution of OBSERVE actions per child across the full sample ($N = 100$), shown for successful and unsuccessful children. (b) Type of action taken at the beginning on the first trial

Figure 5: Behavioral patterns in the Box Task ($N = 100$).

Note that number of observations between LLM agents and children is not directly comparable, as we implemented reliable observations in LLM-based agents, which reveals full information about the box. Figure 6 therefore shows the number of observations made by agents intended as an illustration, not as comparison.

D.2 Task Completion

Children who failed to complete the task accumulated attempts throughout the full 5-minute window without converging on a solution. Such children generally used more attempts compared to successful

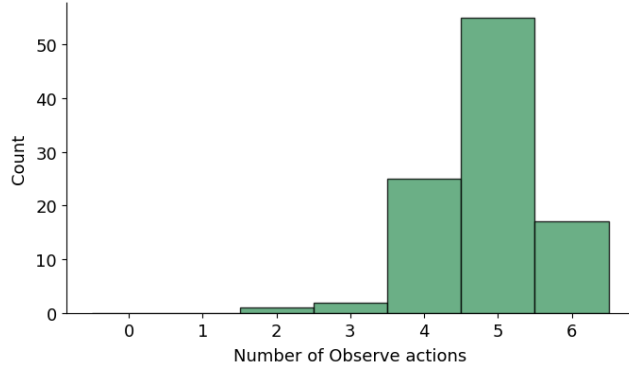


Figure 6: Distribution of OBSERVE actions per simulation ($N = 100$), shows for LLM-PS-P (GPT-5.2, low reasoning).

children. Failure to complete the task consistently reflected reaching a time-out, rather than giving up. (Figure 7).

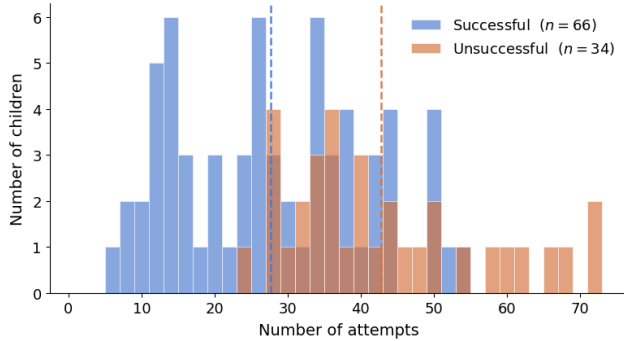


Figure 7: Distribution of attempts at task termination (either all boxes opened or time elapsed) for children who successfully opened all five boxes (blue, $n = 66$) and those who did not (orange, $n = 34$).

D.3 Key Reliability

Figure 8 shows a distribution of empirical key reliability in the Box Task. This is a one-inflated Beta distribution, given by a mixture of:

- A point mass at exactly 1.0: children who got every single "supposed-to-open" attempt right (50%, 50 out of 100 children)
- A continuous $Beta(\alpha, \beta)$ component for the rest, describing children with imperfect success rates (50%, 50 out of 100 children).

MLE fit to the Beta portion estimates `SCIPY.STATS.BETA.FIT` : $\alpha = 5.9, \beta = 2.7$

This distribution model underlies key success rates, used to implement unreliable keys in LLM-PS-S and LLM-PS-P.

D.4 Initial Hypothesis Selection

D.5 Model Fitting Results

Distribution of Success Probabilities on Supposed-to-Open Attempts

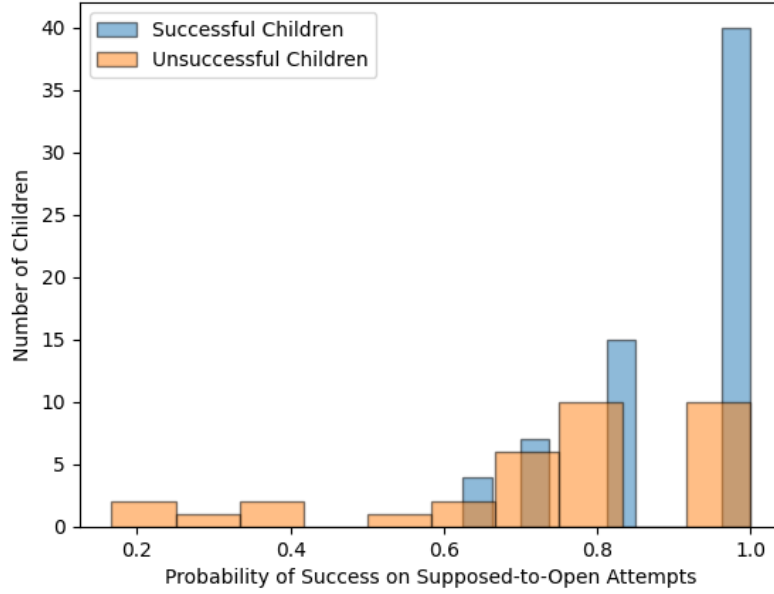


Figure 8: Empirical key reliability in the Box Task. Each bar shows the number of children falling within the given objective reliability bin. (total $N = 100$). Reliability falls below 1.0 for 60% of children, reflecting physical variability in key-lock engagement independent of rule knowledge. This variability motivates the subjective reliability parameter ρ in the SoC model.

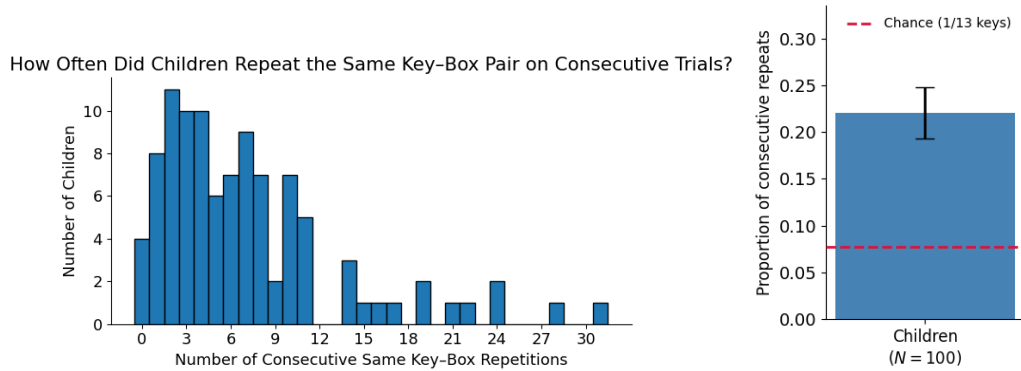


Figure 9: **Left:** Number of consecutive trials on which children ($N = 100$) repeated the same key-box pair. A repeat is defined as attempting the identical key-box combination on trial $t + 1$ as on trial t . **Right:** Proportion of consecutive trials on which children repeated the same key-box pair, aggregated across participants ($N = 100$). Repetitions above chance reflect persistent belief in a hypothesis despite failure, consistent with the subjective reliability account. Error bar indicates 95% bootstrap confidence intervals across participants.

E Code is provided at

<https://anonymous.4open.science/r/Causal-Inference-Under-Uncertainty-BF48/>

F Computational Resources

SoC simulations were run on standard CPU hardware. Each model variant was simulated 100 times per parameter setting; the full grid search (99 settings for SoC-Full) completed in under 20 hours on a single core. LLM-PS experiments used commercial API access to GPT-5.2 (using OpenAI API) and

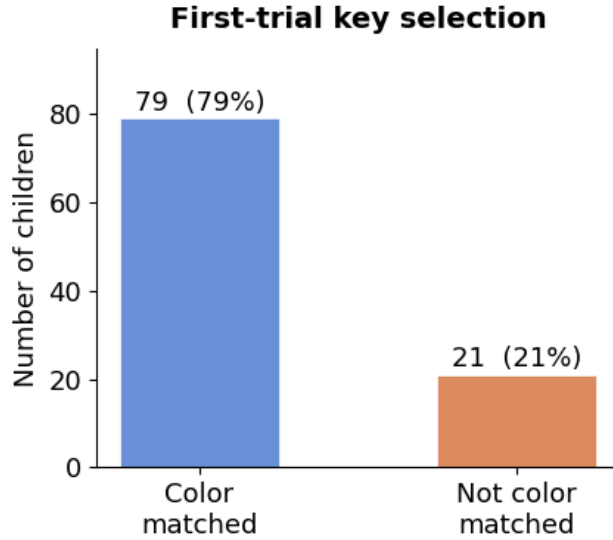
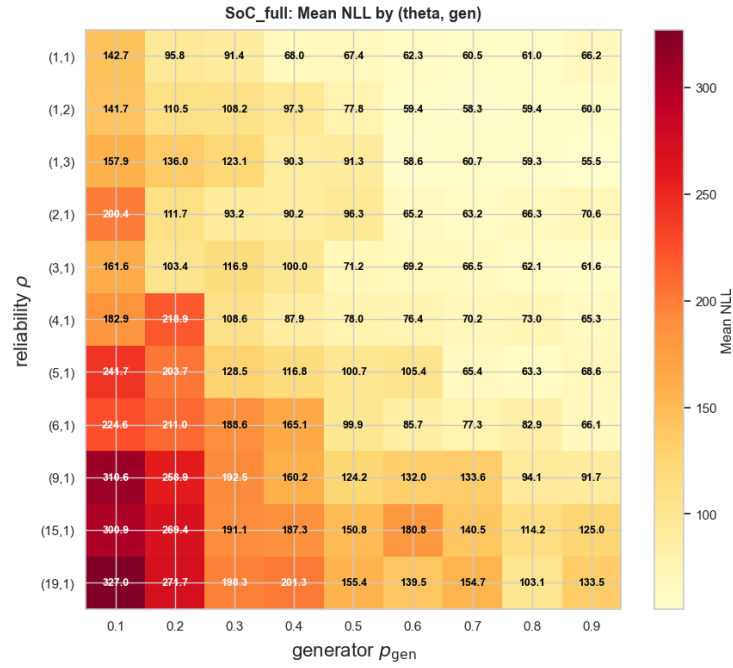


Figure 10: The frequency of first attempt per child across the full sample ($N = 100$) consistent with the taught color-matching rule vs not.

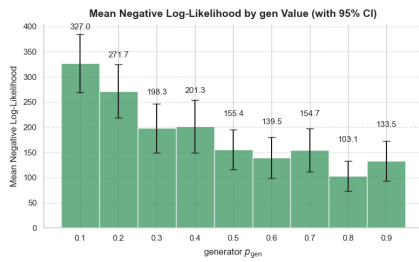
Model	Mean NLL	SD	95% CI	t	p	Cohen's d	
SoC-Lesioned	326.96	295.34	[269.07, 384.84]	10.144	<.001	1.014	***
SoC-Rel	108.61	66.25	[95.62, 121.59]	13.392	<.001	1.339	***
SoC-Gen	100.20	154.11	[70.00, 130.41]	3.897	<.001	0.390	***
SoC-Full	45.89	23.62	[41.26, 50.52]	—	—	—	

Table 5: Model comparison across four SoC variants (NLL, lower = better fit). t -statistics and Cohen's d are from paired t -tests against SoC-Full. $N = 100$ children.

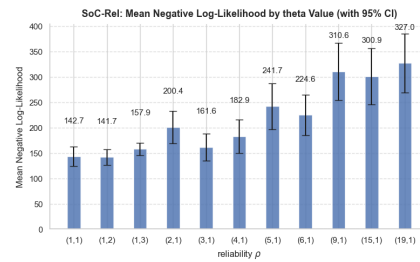
DEEPSEEK V3.2 (using Alibaba cloud API); we have run each variant in under 300 times (including prompt debugging and any live testing during experiments); no GPU resources were required for any experiments reported in this paper.



(a) SoC_full



(b) SoC-Gen



(c) SoC-Rel

Figure 11: Top: SoC-Full parameter fits. NLL values are represented by color heatmap intensity (brighter = better). Bottom: Negative Log-Likelihood for each SoC model variant (shorter=better).

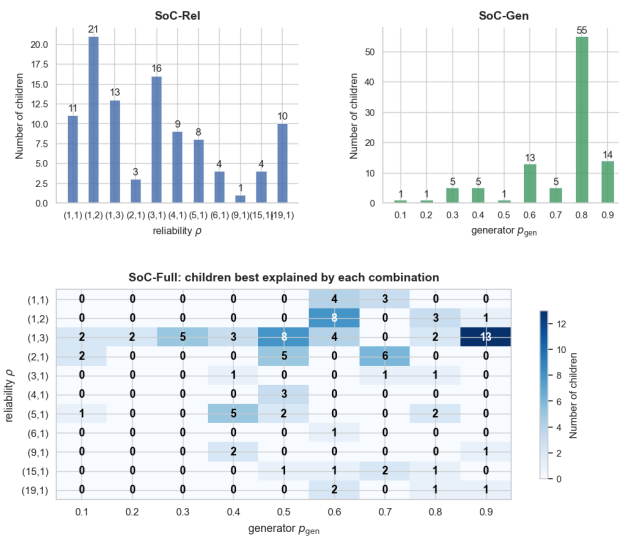


Figure 12: Best-fitting model variant per child. Top row: Bar plots showing the number of children (out of $N = 100$) best explained by each parameter setting, for SoC-Rel and SoC-Gen. Bottom: Heatmap showing the joint distribution of best-fitting parameters for SoC-Full, with two free parameters; cell values indicate the number of children for whom that combination maximised the log-likelihood.